

Copper(I) complex with BINAP and 3,5-dimethylpyrazole: synthesis and photoluminescent properties

Aleksei A. Titov,^a Oleg A. Filippov,^a Alexander F. Smol'yakov,^{a,b,c} Alexey A. Averin^d and Elena S. Shubina^{a*}

^a A. N. Nesmeyanov Institute of Organoelement Compounds, Russian Academy of Sciences, 119991 Moscow, Russian Federation. E-mail: shu@ineos.ac.ru

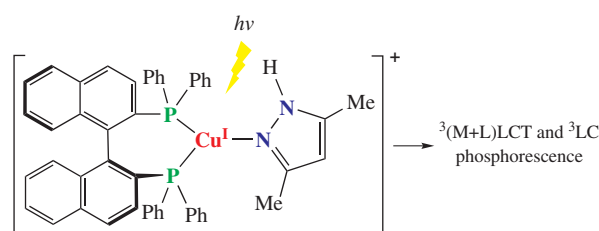
^b Peoples Friendship University of Russia (RUDN University), 117198 Moscow, Russian Federation

^c G. V. Plekhanov Russian University of Economics, 117997 Moscow, Russian Federation

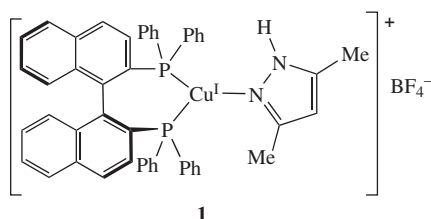
^d A. N. Frumkin Institute of Physical Chemistry and Electrochemistry, Russian Academy of Sciences, 199071 Moscow, Russian Federation

DOI: 10.1016/j.mencom.2019.09.031

A reaction of $[\text{Cu}(\text{MeCN})_4]\text{BF}_4$ with PzH (3,5-dimethylpyrazole) and BINAP [2,20-bis(diphenylphosphino)-1,10-binaphthyl] leads to the formation of mononuclear Cu^{I} complex $[\text{Cu}(\text{PzH})(\text{BINAP})]\text{BF}_4$ containing the molecule of non-deprotonated pyrazole and one BINAP ligand with two phosphorus atoms chelating the metal. This complex exhibits a bright phosphorescence originating from the $^3(\text{M}+\text{L})\text{LCT}$ state at room temperature. At 77 K, the emission is splitted into two components: $^3(\text{M}+\text{L})\text{LCT}$ and ^3LC transitions.



Coordination complexes of Cu^{I} with N- and P-containing donor ligands are of high interest due to their broad structural diversity, divergent catalytic activity,^{1,2} and attractive photophysical properties.^{3,4} Phosphine ligands of different structure play an important role in the coordination chemistry.^{5,6} In this sense, they can stabilize metals in their low oxidation states.⁷ Studies of Cu^{I} complexes bearing the phosphine ligands are often focused on the photophysical characterization. Their attractive luminescent properties are due to the electronic structure of copper centers and the ability to demonstrate thermally activated delayed fluorescence (TADF) features.⁸ On the other hand, the group 11 metals form stable tri-, tetra- and polynuclear complexes with a deprotonated form of pyrazole.^{9–11} In the course of our ongoing investigation of complexes of such metals with pyrazoles and their interaction with electron donors,^{12–14} we have found that the reaction of $[\text{Cu}(\text{MeCN})_4]\text{BF}_4$ with 3,5-dimethylpyrazole (PzH) and 2,20-bis(diphenylphosphino)-1,10-binaphthyl (BINAP) yields mononuclear metal complex $[\text{Cu}(\text{PzH})(\text{BINAP})]\text{BF}_4$ **1** at room temperature in acetone/acetonitrile mixture.[†] It should be noted that the presence of a base (Et_3N) does not lead to the deprotonation of pyrazole and formation of the neutral complex. The obtained compound possesses bright phosphorescence from its $^3(\text{M}+\text{L})\text{LCT}$ and ^3LC states.



X-ray diffraction analysis[‡] revealed that compound **1** is the mononuclear Cu^{I} complex containing one molecule of non-deprotonated dimethylpyrazole coordinated *via* the electron pair of nitrogen atom and one BINAP ligand with two phosphorus atoms chelating the metal (Figure 1).[§] The central environment of Cu atom can be described as a distorted planar triangle, where the additional interaction with a fluorine atom of BF_4^- counterion pulls the Cu atom out of the P(1)N(1)P(2) plane for 0.150 Å. The hydrogen atom of NH group is not involved in any coordination interaction. Copper atom lies also out of $\text{N}_2\text{C}_3\text{Pz}$ plane (by 0.172 Å). The Cu(1)–N(1) bond length in this complex [1.970(2) Å] is comparable to that in the known copper pyrazolate with two coordinated phosphorus atoms^{15,16} and trinuclear Cu^{I} 3,5-dimethylpyrazolate.¹⁷ The Cu(1)–P(1) and Cu(1)–P(2) bonds lengths are 2.533(6) and 2.2596(5) Å, respectively. The N(1)N(2)Cu(1) angle of 123.1(1)° is in the range of MNN angles reported previously for the copper pyrazolate with two coordinated phosphorus atoms.^{15,16}

The crystal packing of this complex is realized due to the quite strong $\text{CH}\cdots\pi$ interactions (shortest $\text{CH}^{\text{Me}}\cdots\text{C}^{\text{Ph}}$ and $\text{CH}^{\text{Ph}}\cdots\text{C}^{\text{Ph}}$ distances being in the range of 2.218–2.893 Å; C–H–C angles for hydrogen atoms of the Me and Ph substituents are 150.82 and 126.92°, respectively). The forced $\text{H}\cdots\text{H}$ and $\text{H}\cdots\text{F}$ contacts were

[‡] Crystals of compound **1** suitable for the X-ray analysis of single crystal were obtained from CH_2Cl_2 /hexane (1 : 2 v/v) solution by slow solvent evaporation at 4 °C.

[§] Crystal data for **1**. $\text{C}_{49}\text{H}_{40}\text{BCuF}_4\text{N}_2\text{P}_2$, monoclinic, space group *Cc*, $a = 20.3340(7)$, $b = 14.9605(5)$ and $c = 14.4148(5)$ Å, $\beta = 109.7790(10)^\circ$, $V = 4126.4(2)$ Å³, $Z = 4$, $d_{\text{calc}} = 1.399$ g cm⁻³, $\mu = 0.663$ mm⁻¹, $R_1 = 0.0263$ [from 11845 unique reflections with $I > 2\sigma(I)$] and $wR_2 = 0.0674$ (from all 45327 unique reflections).

CCDC 1910752 contains the supplementary crystallographic data for this paper. These data can be obtained free of charge from The Cambridge Crystallographic Data Centre *via* <http://www.ccdc.cam.ac.uk>.

[†] See Online Supplementary Materials for the synthetic procedure and characterization of complex **1**.

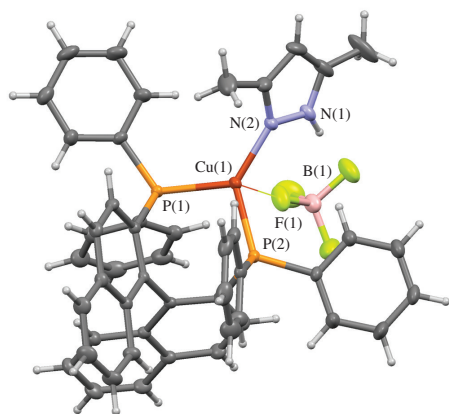


Figure 1 Molecular structure of complex **1** showing thermal ellipsoids at the 50% probability level. Hydrogen atoms are omitted for clarity. Selected bond lengths (Å): Cu(1)–P(1) 2.533(6), Cu(1)–N(1) 1.970(2), Cu(1)–P(2) 2.2596(5), and Cu(1)–F(1) 2.5232(2); bond angles (°): P(1)Cu(1)P(2) 102.07, N(1)Cu(1)P(1) 126.64, and N(1)Cu(1)P(2) 129.76.

also observed. Despite the presence of numerous aromatic substituents, there are no π – π stacking interactions in the structure of the complex.

The electronic spectrum of $[\text{Cu}(\text{PzH})(\text{BINAP})]\text{BF}_4$ in CH_2Cl_2 (Figure 2) contains several intense absorptions in the region that can be assigned to the transitions of $\pi \rightarrow \pi^*$ character (ligand centered, LC) within the BINAP and pyrazole ligands (226 nm, $\epsilon = 2.5 \times 10^5 \text{ dm}^3 \text{ mol}^{-1} \text{ cm}^{-1}$; 250 nm, $\epsilon = 1.5 \times 10^5 \text{ dm}^3 \text{ mol}^{-1} \text{ cm}^{-1}$; 284 nm, $\epsilon = 0.5 \times 10^5 \text{ dm}^3 \text{ mol}^{-1} \text{ cm}^{-1}$; and 325 nm, $\epsilon = 0.18 \times 10^5 \text{ dm}^3 \text{ mol}^{-1} \text{ cm}^{-1}$). There are also broad absorption bands in the region of longer wavelengths (360–420 nm) with a smaller molar extinction coefficient ($\epsilon = 0.01$ – $0.08 \times 10^5 \text{ dm}^3 \text{ mol}^{-1} \text{ cm}^{-1}$), which can be assigned to the charge transfer (CT) transitions. The TD-DFT calculations (performed at the PBE0/def2-SVP level) describe qualitatively the observed UV-VIS spectrum (Table S2, Online Supplementary Materials). The $S_0 \rightarrow S_1$ and $S_0 \rightarrow S_2$ transitions are $(\text{M}+\text{P})\text{L}^{\text{naph}}\text{CT}$ with $f = 0.02$ – 0.04 being the main channels of excitation (Figure 3), which correlates with the data acquired previously for $[\text{Cu}(\text{BINAP})_2]^+$.¹⁸ Notably, the involvement of pyrazole ligand into the highest occupied natural transition orbital (HONTO) of $S_0 \rightarrow S_1$ and $S_0 \rightarrow S_2$ is very small, which means that the nature of this electronic transition is $(\text{Cu}^+ + \text{P}) \rightarrow \text{naphthyl}$, while the pyrazole ligand affects the transition energy. This is in contrast to the copper halide salts, where the halide counterion intensively participates in the electronic transitions.¹⁹

The photoluminescence of complex **1** in the solid state has been studied at room temperature (RT) and 77 K (see Figure 2). The RT emission spectrum displays an intense unstructured broad band (630 nm) with a lifetime belonging to the microsecond domain ($\tau = 5 \mu\text{s}$), which indicates the charge transfer (CT) origin of the

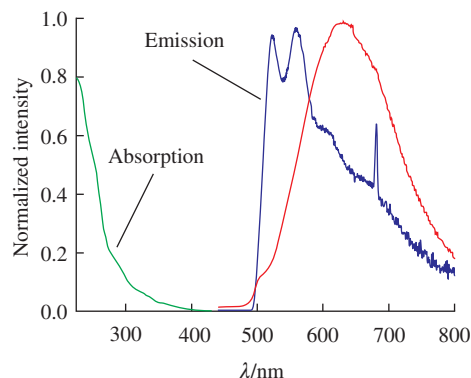


Figure 2 (1) Absorption spectrum of complex **1** in CH_2Cl_2 and normalized emission spectra of a solid sample at (2) RT and (3) 77 K ($c = 3 \times 10^{-5} \text{ mol dm}^{-3}$).

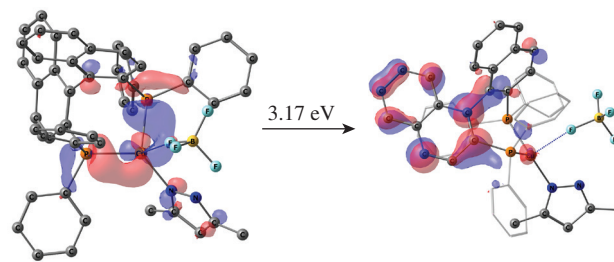


Figure 3 HONTO and LUNTO for the $S_0 \rightarrow S_1$ transition in complex **1**.

observed emission, *i.e.*, the phosphorescence.^{18,19} Cooling the sample down to 77 K leads to the emission splitting into two components (see Figure 2). One of them (tail around 660 nm, $\tau = 176 \mu\text{s}$) can be assigned to the red-shifted RT emission that additionally confirms its $^3(\text{M}+\text{P})\text{LCT}$ origin. High-energy bands (525, 560 and shoulder at 610 nm, $\tau = 2600 \mu\text{s}$) are typical of the ^3LC transitions within bis-naphthyl derivatives.^{19,20} It should be noted that the triplet state decay at low temperature can be only fitted according to the bi-exponential analysis with a nearly equal contribution of the microsecond and millisecond components due to the extensive overlapping of emission bands.

In conclusion, we have synthesized a new type of the Cu^{I} complex with non-deprotonated pyrazole and chelating bisphosphine. This complex possesses a bright photoluminescence in the solid state. The main excitation channels are $(\text{M}+\text{P})\text{L}^{\text{naph}}\text{CT}$ transitions. The coordination of dimethylpyrazole to the metal atom affects mainly the energy of $(\text{Cu}^+ + \text{P}) \rightarrow \text{naphthyl}$ transition in contrast to the halide ligands/counterions. At room temperature, this complex exhibits the orange phosphorescence originating from $^3(\text{M}+\text{P})\text{LCT}$ states. The temperature decrease to 77 K leads to the emission splitting into two components: the phosphorescence originating from the charge transfer ($\tau = 176 \mu\text{s}$) state and the more intense greenish long-lived naphthalene ligand-centered ($\tau = 2600 \mu\text{s}$) state.

This work was supported in parts of the synthesis and characterization of compounds and calculations by the Russian Science Foundation (grant no. 17-73-10369). The elemental analysis was supported by the Ministry of Science and Higher Education of the Russian Federation and was performed using the equipment of the Center for Molecular Composition Studies at the A. N. Nesmeyanov Institute of Organoelement Compounds of the Russian Academy of Sciences. The photophysical properties were estimated using the equipment of the Center of Physical Methods of Investigation at the A. N. Frumkin Institute of Physical Chemistry and Electrochemistry of the Russian Academy of Sciences. The X-ray analysis carried out by A. F. Smol'yakov was supported by the Peoples Friendship University of Russia (university program '5-100').

Online Supplementary Materials

Supplementary data associated with this article can be found in the online version at doi: 10.1016/j.mencom.2019.09.031.

References

- 1 *Metal-Catalyzed Cross-Coupling Reactions*, eds. A. de Meijere and F. Diederich, Wiley-VCH, Weinheim, 2004.
- 2 F. A. Arteaga, Z. Liu, L. Brewitz, J. Chen, B. Sun, N. Kumagai and M. Shibasaki, *Org. Lett.*, 2016, **18**, 2391.
- 3 A. Barbieri, G. Accorsi and N. Armaroli, *Chem. Commun.*, 2008, 2185.
- 4 Y. Liu, S.-C. Yiu, C.-L. Ho and W.-Y. Wong, *Coord. Chem. Rev.*, 2018, **375**, 514.
- 5 A. A. Karasik, A. S. Balueva, E. I. Musina and O. G. Sinyashin, *Mendeleev Commun.*, 2013, **23**, 237.
- 6 Y. Zhang, M. Schulz, M. Wächter, M. Karnahl and B. Dietzek, *Coord. Chem. Rev.*, 2018, **356**, 127.

- 7 D. G. Cuttell, S.-M. Kuang, P. E. Fanwick, D. R. McMillin and R. A. Walton, *J. Am. Chem. Soc.*, 2002, **124**, 6.
- 8 R. Czerwieńiec, M. J. Leidl, H. H. H. Homeier and H. Yersin, *Coord. Chem. Rev.*, 2016, **325**, 2.
- 9 K. Fujisawa, Y. Ishikawa, Y. Miyashita and K.-I. Okamoto, *Inorg. Chim. Acta*, 2010, **363**, 2977.
- 10 A. A. Titov, A. F. Smol'yakov, A. N. Rodionov, I. D. Kosenko, E. A. Guseva, Ya. V. Zubavichus, P. V. Dorovatovskii, O. A. Filippov and E. S. Shubina, *Russ. Chem. Bull., Int. Ed.*, 2017, **66**, 1563 (*Izv. Akad. Nauk, Ser. Khim.*, 2017, 1563).
- 11 D. N. Bazhin, Yu. S. Kudyakova, P. A. Slepukhin, Ya. V. Burgart, N. N. Malysheva, A. N. Kozitsina, A. V. Ivanova, A. S. Bogomyakov and V. I. Saloutin, *Mendeleev Commun.*, 2018, **28**, 202.
- 12 A. A. Titov, O. A. Filippov, A. F. Smol'yakov, K. F. Baranova, E. M. Titova, A. A. Averin and E. S. Shubina, *Eur. J. Inorg. Chem.*, 2019, 821.
- 13 A. A. Titov, A. F. Smol'yakov, K. F. Baranova, O. A. Filippov and E. S. Shubina, *Mendeleev Commun.*, 2018, **28**, 387.
- 14 A. A. Titov, O. A. Filippov, L. M. Epstein, N. V. Belkova and E. S. Shubina, *Inorg. Chim. Acta*, 2018, **470**, 22.
- 15 C. Pettinari, F. Marchetti, R. Polimante, A. Cingolani, G. Portalone and M. Colapietro, *Inorg. Chim. Acta*, 1996, **249**, 215.
- 16 L. N. Bochkarev, Y. P. Bariniva, A. I. Ilicheva, S. Y. Ketkov, E. V. Baranov, V. A. Ilichev and D. G. Yakhvarov, *Inorg. Chim. Acta*, 2015, **425**, 189.
- 17 J. He, Y.-G. Yin, T. Wu, D. Li and X.-C. Huang, *Chem. Commun.*, 2006, 2845.
- 18 X. Zarate, E. Schott, R. Ramirez-Tagle, D. MacLeod-Carey and R. Arratia-Pérez, *Polyhedron*, 2012, **37**, 54.
- 19 H. Kunkely, V. Pawlowski and A. Vogler, *Inorg. Chem. Commun.*, 2008, **11**, 1003.
- 20 H. Kunkely and A. Vogler, *Inorg. Chem. Commun.*, 2006, **9**, 866.

Received: 17th April 2019; Com. 19/5891